frontiers
in Immunology

The Role of Conformational Dynamics in Antigen Trimming by Intracellular Aminopeptidases

Athanasios Papakyriakou[1,2]* and Efstratios Stratikos[2]*

[1]Centre for Biological Sciences, Faculty of Natural and Environmental Sciences, University of Southampton, Southampton, United Kingdom, [2]National Centre for Scientific Research "Demokritos", Athens, Greece

Antigenic peptides presented by the major histocompatibility complex class I (MHC-I) molecules for recognition by cytotoxic T-lymphocytes are processed by members of the oxytocinase sub-family of M1 aminopeptidases ERAP1, ERAP2, and IRAP. These three homologous zinc metallopeptidases trim N-terminally extended precursor antigenic peptides down to the correct length for loading onto the MHC-I but can also destroy some antigenic peptides by over-trimming, therefore, influencing the antigenic peptide repertoire and immunodominance hierarchy. Polymorphic variation has been found to affect their trimming function and predispose to human disease in complex and poorly understood patterns. Structural and biochemical analysis have pointed toward a complicated trimming mechanism that involves a major conformational transition during each catalytic cycle. Here, we provide an overview of current knowledge on the structure and mechanism of action of those enzymes with a focus on the proposed key role of conformational dynamics in their function.

Keywords: ERAP1, ERAP2, IRAP, conformational dynamics, antigenic peptide trimming, molecular dynamics simulations, X-ray structural analysis

BIOLOGICAL FUNCTION

The adaptive immune system relies on the presentation of peptides generated by processing of intracellular and endocytosed proteins on the cell surface for surveillance by cytotoxic T-lymphocytes. Peptides generated in the cytosol are transferred into the ER through the transporter associated with antigen processing, TAP (1, 2), where they bind to nascent major histocompatibility complex class I (MHC-I) molecules. The C-terminal residues of these peptides generally match the sequence requirements of MHC-I; however, the optimum length of 8–10 residues for MHC-I alleles requires some N-terminal processing. This key step of antigenic peptide optimization is performed by a group of homologous enzymes that belong to the M1 family of zinc-dependent aminopeptidases: the ER-resident aminopeptidases ERAP1 and ERAP2, and the endosomal insulin-regulated aminopeptidase IRAP (3). Human ERAP1 (941 aa, 107 kDa) also known as ARTS-1 and adipocyte-derived leucine aminopeptidase (A-LAP) and ERAP2 (960 aa, 110 kDa), also known as leukocyte-derived arginine aminopeptidase (L-RAP), share a sequence identity of 51%. IRAP (1025 aa, 117 kDa) also known as leucyl-cystinyl aminopeptidase and placental leucine aminopeptidase is a transmembrane enzyme with sequence identity of 46% for ERAP1 and 44% for ERAP2, which comprises an additional 109 aa N-terminal cytosolic domain for targeting to intracellular vesicles (4). In humans, these three aminopeptidases are encoded in a 200 kb segment on chromosome 5q15, whereas rodents

express only an ERAP1 homolog (aminopeptidase associated with antigen processing, ERAAP) and IRAP.

The importance of antigenic precursor trimming in the MHC-I antigen-processing pathway was consolidated by the discovery of ERAAP (5, 6) and subsequently by evidence that ERAAP-deficient mice display disruptions in their peptide–MHC-I repertoire (7–10). But even before the identification of ERAAP, several models describing synergy between MHC-I and protease activity in the ER had been proposed (11–13). According to these models, the MHC I could either serve as template to guide peptide proteolytic processing while it is bound onto the MHC-I, or control proteolytic processing of the peptide indirectly, by binding and protecting from excessive proteolysis antigenic peptides generated in solution. ERAP1 (as well as ERAP2 and IRAP) belongs to the well-studied M1 family of aminopeptidases, enzymes that are known to efficiently trim peptides in solution (14). Furthermore, initial analysis suggested that ERAP1 has some unique enzymatic properties that were consistent with its specialization of antigenic peptides: specifically, it was found to show some selectivity for sequence and most notably for length (termed the "molecular ruler" mechanism), processing effectively large antigenic peptide precursors and sparing peptides 8–9 amino acids long, the usual length for antigenic peptides (15–17). On the other hand, several studies have provided evidence that ERAP1 can trim N-terminally extended antigenic peptide precursors while they are bound onto MHC-I, allowing the sequence selectivity of the MHC-I to determine the generation of the antigenic peptide repertoire (7, 18). This model has been supported by recent studies demonstrating that ERAAP (19) and ERAP1–ERAP2 heterodimers (20) can trim antigenic precursors that are disulfide-linked as single-chain MHC-I trimers. In another study, however, the authors found that a specific MHC allele was only able to protect, rather than guide, elongated antigenic peptide precursors from ERAP1 degradation (21). Although these two models of aminopeptidase-assisted antigenic peptide generation are not necessarily mutually exclusive and may operate in parallel, they do shift the burden of selectivity between the MHC-I and the enzyme and as a result have important implications in our understanding of the basic mechanisms behind the generation of the immunopeptidome. Unfortunately, no direct comparison of the trimming rates of ERAP for peptides in solution or bound onto MHC-I have been performed yet, making the evaluation of the relative importance of these two processes speculative for the moment.
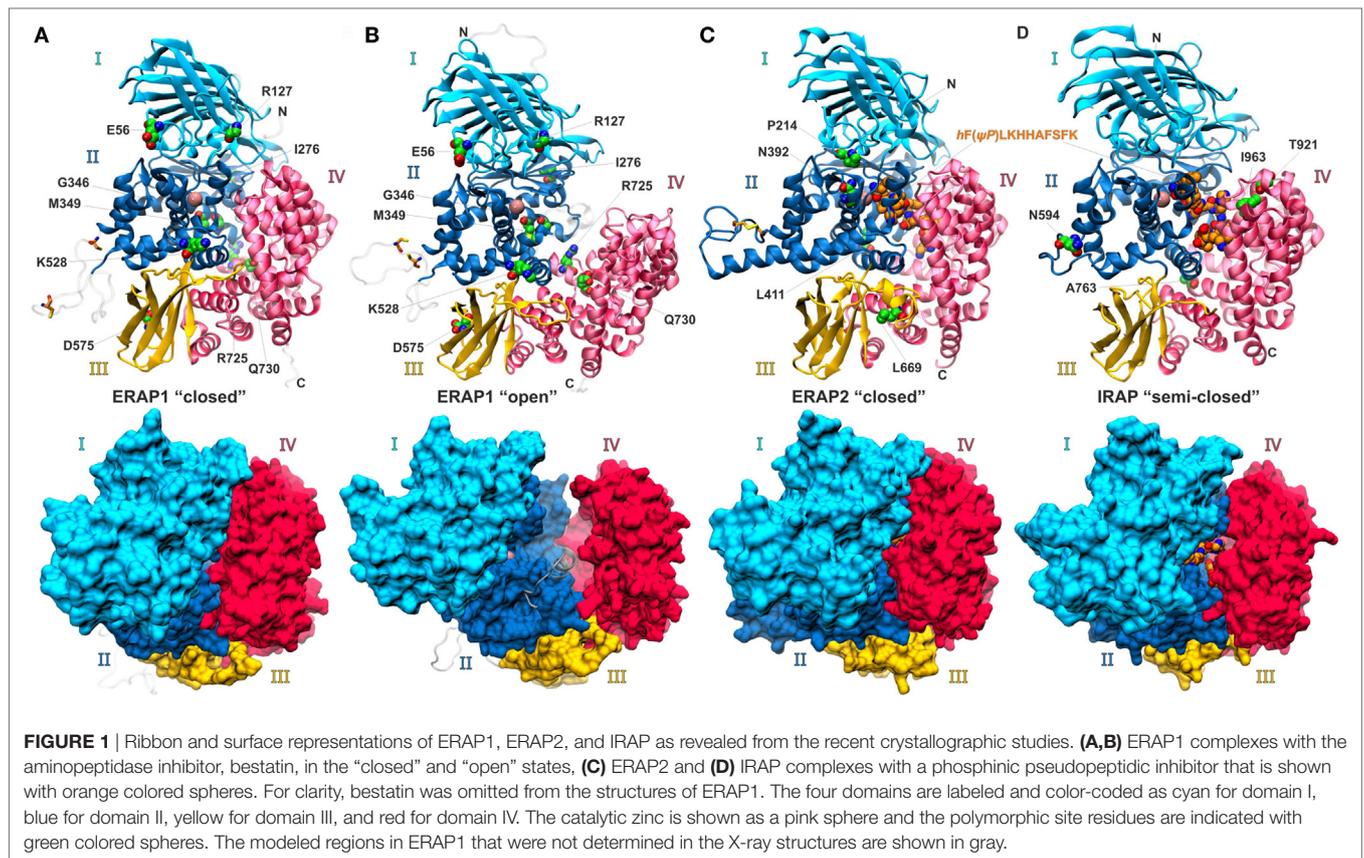
Over the last 6 years, a series of crystallographic studies of the three antigen processing enzymes have revealed a wealth of information that promotes our understanding of their substrate specificity and peptide trimming at the molecular level (22). Although, these structures have significantly enhanced our understanding of the mechanism of soluble peptide trimming, they have provided little insight on how a relatively short peptide can be trimmed while bound onto MHC-I. At the same time, however, they have established a structural framework that points to a great degree of conformational flexibility for ERAP1 and homologous enzymes. Computational approaches such as molecular dynamics simulations have recently been used to better understand this conformational flexibility and

to formulate structural perspectives on the mechanisms of antigenic peptide trimming.

OVERALL STRUCTURE AND CONFORMATIONAL CHANGES

The X-ray structures of ERAP1 in complex with a general aminopeptidase inhibitor, bestatin, were the first to be determined by two independent groups (17, 23). These studies revealed that the enzyme can adopt two distinct conformations: a "closed" conformation where substrate entrance into a large internal cavity that includes the catalytic site is occluded (**Figure 1A**), and a set of closely related "open" conformational states where the catalytic site is solvent exposed (**Figure 1B**). Shortly after, the structure of ERAP2 with a zinc-bound lysine residue in the active site was determined in the "closed" conformation (24). ERAP2 has been also crystallized in the presence of two phosphinic pseudopeptides, a tripeptide (25), and a decapeptide (26) analog, which mimic the transition state of a bound substrate (**Figure 1C**). So far, no structure of ERAP2 has been obtained in an "open" state. However, during the last 2 years, crystal structures of IRAP have been solved in the presence of alanine and lysine zinc-bound products (27), as well as in a ligand-free form and in complex with the aforementioned phosphinic decapeptidic analog (28). Remarkably, all these structures displayed IRAP in an intermediate conformation between the "closed" and "open" states of ERAP1, henceforth referred to as "semi-closed" (**Figure 1D**). Recently, a "closed" conformation of IRAP has also been solved by X-ray crystallography (29). This conformation was apparently induced by binding of a selective potent inhibitor, exhibited structural changes in the active site loop containing the conserved exo-peptidase G-A-M-E-N motif and was overall very similar to the "closed" conformations of ERAP1 and ERAP2, suggesting that it may constitute the active conformation of the enzyme. It should be noted that this conformational plasticity is not unique to ERAP1 or IRAP, but seems to extend to other members of the M1 family of aminopeptidases since structures of the tricorn-interacting factor F3 (30) and aminopeptidase N (APN) (31) have also revealed closed, intermediate and open conformations.

As members of the oxytocinase subfamily of M1 aminopeptidases (3), the structures of ERAP1, ERAP2, and IRAP comprise of four domains (**Figure 1**). Domain I comprises three β-sheets that pack against the catalytic domain II and interacts with the C-terminal domain IV in the "closed" state. The thermolysin-like domain II contains the characteristic **H**EXX**H**(X)$_{18}$**E** zinc-binding motif and the exo-peptidase-specific GAMEN motif, which creates one edge of the substrate-binding cleft. The N-terminal cleft of the substrate-binding region is blocked by domain I and can anchor the N-terminal amine group of the peptides *via* two conserved glutamic acid residues. Domain III is composed of two β-sheets that form a beta-sandwich and acts as a lever that pulls domain IV away from the catalytic active site providing access to substrates in the "open" states. The bowl-shaped domain IV consists of only α-helices in an antiparallel topology and forms an arch over domain II that seals off the active site in the
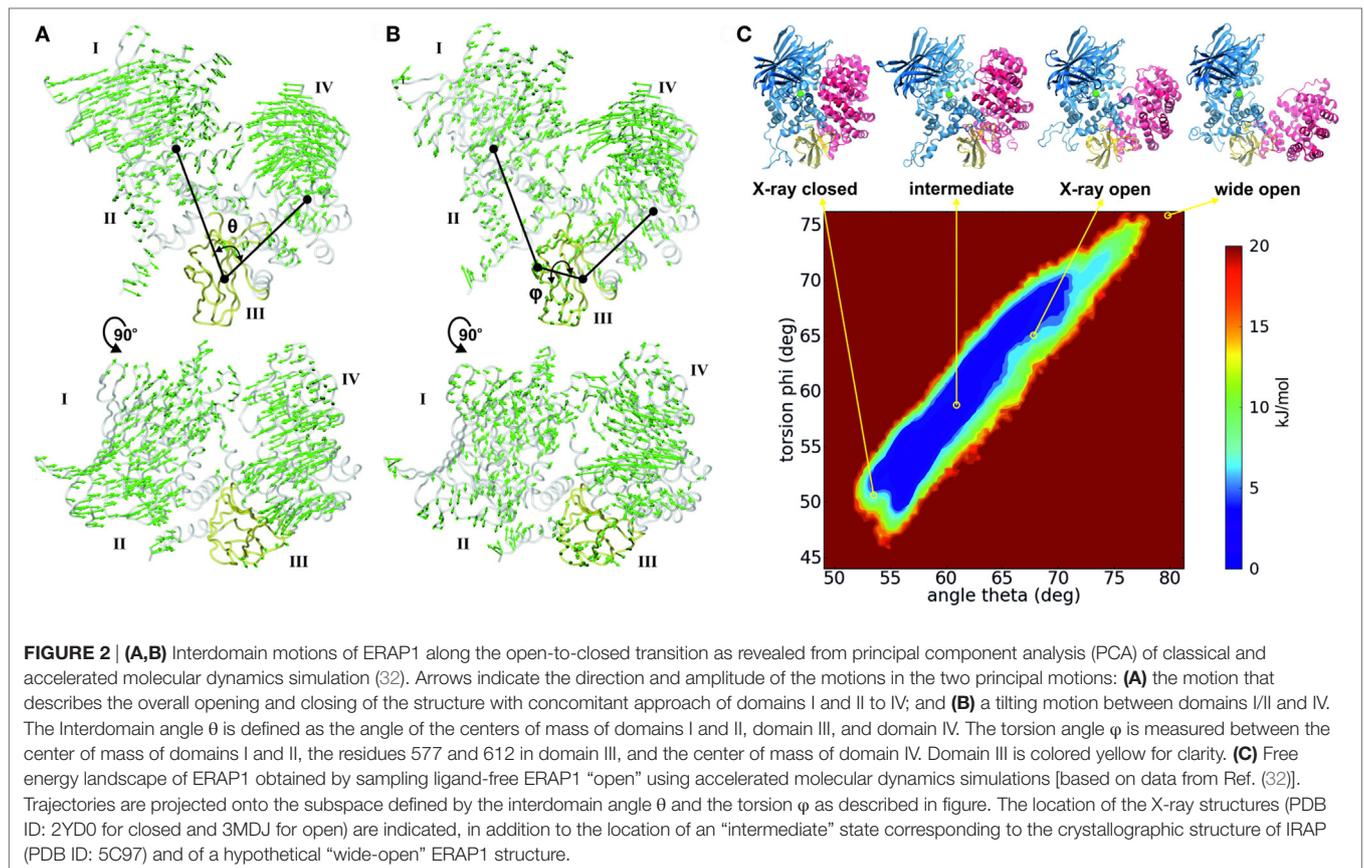
FIGURE 1 | Ribbon and surface representations of ERAP1, ERAP2, and IRAP as revealed from the recent crystallographic studies. **(A,B)** ERAP1 complexes with the aminopeptidase inhibitor, bestatin, in the "closed" and "open" states, **(C)** ERAP2 and **(D)** IRAP complexes with a phosphinic pseudopeptidic inhibitor that is shown with orange colored spheres. For clarity, bestatin was omitted from the structures of ERAP1. The four domains are labeled and color-coded as cyan for domain I, blue for domain II, yellow for domain III, and red for domain IV. The catalytic zinc is shown as a pink sphere and the polymorphic site residues are indicated with green colored spheres. The modeled regions in ERAP1 that were not determined in the X-ray structures are shown in gray.

"closed" state. The internal cavities of the closed conformations of ERAP1/2 and IRAP have an approximate volume of 2,900 Å³, which is larger than those found in other M1 aminopeptidases, like ePepN (2,200 Å³) and LTA4 (1,130 Å³). Notably, the crystal structure of IRAP in the "semi-open" conformation displayed a much larger internal cavity of approximately 5,300 Å³ volume, an observation that is consistent with IRAP's unique ability to bind and cleave cyclic peptides (27, 28).

The "closed" and "open" crystal structures of ERAP1 demonstrated that main conformational change of the enzyme is the movement of domain IV relative to domains I and II (17, 23). However, examination of the active sites residues revealed key structural reorganization possibly associated with the mechanism of peptide hydrolysis. A highly conserved tyrosine residue among M1 aminopeptidases (Tyr438 in ERAP1, Tyr455 in ERAP2, and Tyr549 in IRAP) that interacts with the carbonyl group of the scissile peptide bond was found to move away from the active site in the "open" state. The importance of this residue for catalysis led to the suggestion that domain closure is linked to the catalytic mechanism. Indeed, a tyrosine to phenylalanine substitution at position 433 of ERAP1 caused a 200-fold reduction in the catalytic rate of L-AMC hydrolysis (17). In the ligand-occupied closed conformations of ERAP2 and IRAP, the equivalent tyrosine residue adopted a similar orientation as in the closed ERAP1 structure (26, 29). In contrast, in the ligand-free forms of ERAP2 and IRAP, the catalytic tyrosine adopted intermediate positions (26, 28).

Recent experimental analysis of the solution structure of ERAP1 using small-angle X-ray scattering (SAXS) revealed that, in solution, the average structure of ERAP1 corresponds well with the crystallographically observed open conformation (32). This analysis was performed with ligand-free enzyme and is, therefore, consistent with the proposal that "open" ERAP1 is the substrate-capture conformation and that substrate binding promotes the conformational shift to "closed" ERAP1 that facilitates catalysis (17, 29). Further structural analysis using different ligands, substrate analogs, or inhibitors will be necessary to unequivocally support this hypothesis.

STRUCTURAL DYNAMICS OF ERAP1

The recent advances in enhanced sampling computational methods combined with the power of graphics processing units has allowed the sampling of large conformational changes that occur in the microsecond to millisecond time scale (33), such as the open-to-closed transition of ERAP1. Analysis using classical and accelerated molecular dynamics revealed that the conformational changes in ERAP1 revolve around two main components (**Figures 2A,B**), which can be described by: (i) a scissor motion around a pivot point that corresponds to domain III (hinge domain) and varies the distance between domains I/II and IV and (ii) a tilting motion between domains I/II and IV that can affect their relative orientation (32, 34). These motions can be described using two simple, collective variables;

FIGURE 2 | (A,B) Interdomain motions of ERAP1 along the open-to-closed transition as revealed from principal component analysis (PCA) of classical and accelerated molecular dynamics simulation (32). Arrows indicate the direction and amplitude of the motions in the two principal motions: (A) the motion that describes the overall opening and closing of the structure with concomitant approach of domains I and II to IV; and (B) a tilting motion between domains I/II and IV. The Interdomain angle θ is defined as the angle of the centers of mass of domains I and II, domain III, and domain IV. The torsion angle φ is measured between the center of mass of domains I and II, the residues 577 and 612 in domain III, and the center of mass of domain IV. Domain III is colored yellow for clarity. (C) Free energy landscape of ERAP1 obtained by sampling ligand-free ERAP1 "open" using accelerated molecular dynamics simulations [based on data from Ref. (32)]. Trajectories are projected onto the subspace defined by the interdomain angle θ and the torsion φ as described in figure. The location of the X-ray structures (PDB ID: 2YD0 for closed and 3MDJ for open) are indicated, in addition to the location of an "intermediate" state corresponding to the crystallographic structure of IRAP (PDB ID: 5C97) and of a hypothetical "wide-open" ERAP1 structure.

the inter-domain angle θ, and the torsion angle φ, respectively (**Figures 2A,B**).

Although complete sampling of the structural dynamics of ERAP1 is an insurmountable computational task, projection of the trajectories obtained from molecular dynamics simulations onto the θ/φ subspace revealed a multi-basin energy landscape with distinct conformational states of comparable Boltzmann probabilities (**Figure 2C**). Closed states (θ = 50–55°), intermediate states (θ = 55–65°), and open states (θ = 65–70°) are accessible to ligand-free ERAP1 within low energy barriers. Even more open conformations of ERAP1 (θ > 75°) that expose the catalytic center of the enzyme to the solvent can be sampled, albeit with a higher energetic cost. Such conformational states could be relevant for peptide trimming onto MHC-I (*vide supra*).

The nature of the described conformational changes suggests that interactions between domains II and IV may affect the enzymatic efficiency and mechanism of the enzyme. A recent study investigated the role of such interactions by using site-directed mutagenesis to perturb key salt bridge interactions formed between domains I/II and IV in the "closed" state of ERAP1 (32). Although the mutations were located far away from the active site and the peptide binding groove, the disruption of these salt-bridges reduced the catalytic efficiency at low substrate concentrations and enhanced the allosteric kinetic behavior of ERAP1. Small-angle X-ray scattering analysis and molecular dynamics simulations suggested that disruption of these salt bridges increases the energetic barrier toward the "closed" state, thus

affecting the catalytic efficiency of ERAP1 indirectly. This study provided additional evidence supporting the link between the conformational change in ERAP1 and its enzymatic mechanism.

ERAP1 POLYMORPHISMS AND MOLECULAR DYNAMICS

A multitude of genome-wide association studies during the last decade have provided evidence that several coding single nucleotide polymorphisms (SNPs) in the genes of ERAP1 and ERAP2 are linked with predisposition to human disease. The most pronounced example is the association of ERAP1 SNPs with ankylosing spondylitis (35, 36), a highly heritable, inflammatory disease with autoimmune etiology that is closely associated with the HLA-B*27 allele. Epistasis between ERAP1 SNPs and HLA alleles further validated the functional significance of those findings (37). In addition, ERAP1 is associated with juvenile idiopathic arthritis (38) and Behçet disease (39), whereas ERAP2 is associated with Crohn's disease (40) and birdshot chorioretinopathy (41). Notably, both ERAP1 and ERAP2 have been associated with psoriasis (42, 43), a chronic autoimmune inflammatory disease that has also been associated with an IRAP coding SNP (44). There are also accumulating evidence that the polymorphic variation in these enzymes may contribute to predisposition to cancer (45, 46).

Several functional studies have demonstrated that these disease-associated SNPs lead to altered enzymatic activity, antigen
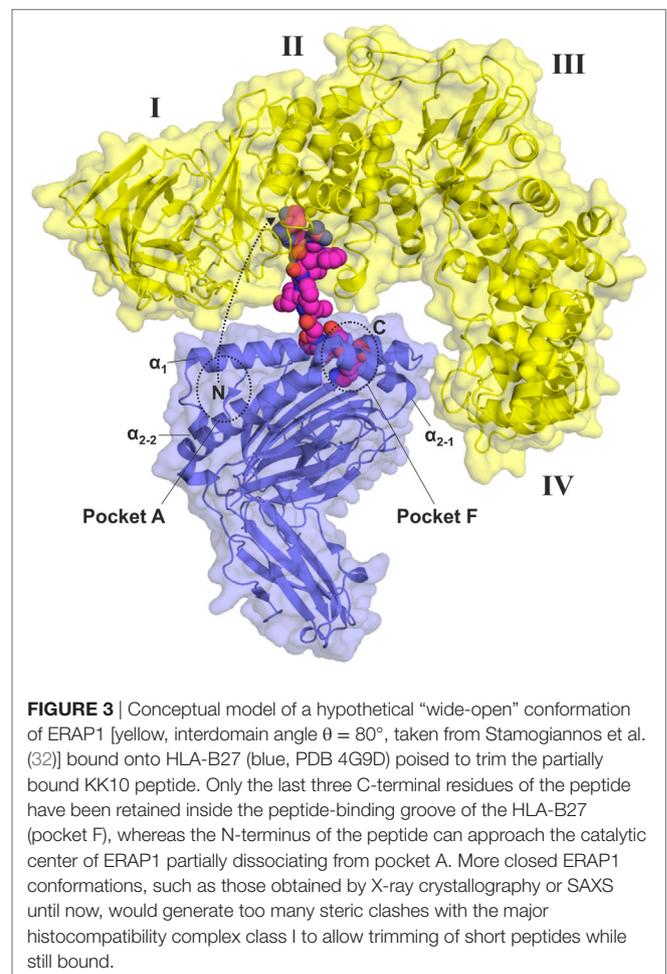
presentation, and cytotoxic responses (47–51). In particular, distinct ERAP1 haplotypes have been grouped as "normal," "hypofunctional," or "hyperfunctional" in terms of their ability to generate specific antigenic epitopes (19). Mapping these SNPs on the crystallographic structures revealed that most of the polymorphic sites are located distally from the active site and thus their effect in the catalytic activity cannot be readily inferred. One exception is the rs2549782 SNP of ERAP2 that codes for the variation N392K, which resides adjacent to the substrate N-terminus-binding cleft (**Figure 1C**). After obtaining the crystal structures of both ERAP2 variants, a structural comparison revealed that the side-chain of 392 assumes different orientations (49). In particular, K392 was oriented toward the N-terminal amine group of the bound product, introducing a highly unfavorable electrostatic interaction with the substrate, which could interfere with transition-state stabilization resulting in reduced catalytic efficiency. This substitution also led to rearrangement of residues around the S1 specificity pocket that may explain the changes in the specificity profiles of two alleles (49).

The two most common disease-associated ERAP1 SNPs are rs30187 that codes for the K528R variant, and rs27044 that codes for Q730E. Both these SNPs have been repeatedly shown to affect the enzymatic activity of ERAP1. In particular, the 528R variant displays lower enzymatic activity compared to 528K, whereas the 730E variant affects both activity but also the length preference toward shorter peptides (34, 47, 50, 51). Given that position 730 lies within the internal cavity of ERAP1, which is in close proximity to a site that has been proposed as a regulatory region (52, 53), the effect of this polymorphism can be rationalized by the influence of the negative charge introduced by the Q730E change on the C-terminus of long substrates (34). However, this is not the case for the solvent exposed position 528 that has no direct access to the peptide-binding cavity (**Figures 1A,B**). It has been proposed that the nature of the amino acid at position 528 can affect the structural dynamics of the hinge domain III and, therefore, indirectly influence the dynamic equilibrium between the "open" and "closed" states of ERAP1. This hypothesis was explored by a comparative analysis of the dynamics of ancestral ERAP1 and its 528R and 730E variants using molecular dynamics simulations (34). These simulations suggested that while the 730E variant samples approximately the same conformational space as the native ERAP1, the 528R variant is limited to more "semi-closed" configurations, as those displayed by the X-ray structures of IRAP (**Figure 1D**). Considering that substrate access is more limited in "semi-closed" conformations, a perturbation of the conformational equilibrium in the 528R variant could explain its reduced activity.

ERAP1 CONFORMATIONAL DYNAMICS AND PEPTIDE TRIMMING ONTO MHC-I

Although the crystallographic structures of ERAP1 along with conformational analysis provided by molecular dynamics simulations provide a solid framework for understanding the mechanism that the enzyme uses to trim peptides in solution, structural insight on the proposed function of ERAP1 to trim peptides while bound onto MHC-I has been more elusive (20).

Indeed, upon solving the first crystallographic structures of ERAP1, which featured a structural topology very similar to all other enzymes of the M1 family of aminopeptidases, it became obvious that the capability of a MHC-I partially bound peptide to approach the catalytic site of ERAP1 would be severely hindered by steric clashes between ERAP1 and the MHC-I. Initial modeling using the "open" crystallographic structure of ERAP1 suggested that the peptide would need to be at least 16 residues long to reach into the active site of ERAP1 while still retaining some limited but meaningful interactions with the MHC-I (17). Recent analysis using SAXS has confirmed that the solution structure of ERAP1 corresponds well to this "open" conformation, raising the question on how ERAP1 could possibly trim an MHC-I bound peptide down to the final epitope of 8–9 amino acids long. On the other hand, however, molecular dynamics simulations suggest that more open conformations of ERAP1 are structurally accessible although of higher energy (**Figure 3**). It is therefore possible that intramolecular interactions with the MHC-I could stabilize such conformations to allow for closer approach and peptide trimming. Although ERAP1 has been suggested to be mostly inactive in the "open" states, it may still have some enzymatic activity since even the Tyr433Phe ERAP1 mutant retains some activity (17). Furthermore, the reduction in the catalytic

FIGURE 3 | Conceptual model of a hypothetical "wide-open" conformation of ERAP1 [yellow, interdomain angle θ = 80°, taken from Stamogiannos et al. (32)] bound onto HLA-B27 (blue, PDB 4G9D) poised to trim the partially bound KK10 peptide. Only the last three C-terminal residues of the peptide have been retained inside the peptide-binding groove of the HLA-B27 (pocket F), whereas the N-terminus of the peptide can approach the catalytic center of ERAP1 partially dissociating from pocket A. More closed ERAP1 conformations, such as those obtained by X-ray crystallography or SAXS until now, would generate too many steric clashes with the major histocompatibility complex class I to allow trimming of short peptides while still bound.

rate of ERAP1 in an "open" conformation could be compensated by the high local enzyme-substrate concetrations achieved as a consequence of ERAP1 binding onto MHC-bound peptides. A conceptual theoretical model of such an interaction is shown in **Figure 3**. It should be noted, however, that to date, no such conformations have been observed experimentally nor any direct ERAP1–MHC-I interactions demonstrated. Further enzymatic and biophysical analysis will be necessary to provide structural support to this model of ERAP1 action.

CONCLUSION—PERSPECTIVES

In summary, we have reviewed the up-to-date structural data on the conformational plasticity of three key aminopeptidases that generate antigenic peptides for presentation by MHC-I. Overall, structural and enzymatic analysis point to a complex mechanism of peptide trimming that involves a cycle between several conformational states. Understanding the molecular dynamics of these conformational changes is emerging as a

powerful approach to explain the physiological functions of these enzymes as well as the complicated effects of disease-associated coding SNPs that are located away from the catalytic site. Translation of this structural plasticity to the enzyme's active site can also affect inhibitor binding, making computational molecular dynamics approaches invaluable for inhibitor optimization efforts. Conformational dynamics may be the key to fully understanding the mechanism of antigenic peptide trimming by ERAP1 and homologous aminopeptidases.

AUTHOR CONTRIBUTIONS

Both authors contributed equally to all sections of the manuscript.

FUNDING

REFERENCES

1. Lehnert E, Tampe R. Structure and dynamics of antigenic peptides in complex with TAP. *Front Immunol* (2017) 8:10. doi:10.3389/fimmu.2017.00010
2. van Endert PM, Tampe R, Meyer TH, Tisch R, Bach JF, McDevitt HO. A sequential model for peptide binding and transport by the transporters associated with antigen processing. *Immunity* (1994) 1(6):491–500. doi:10.1016/1074-7613(94)90091-4
3. Tsujimoto M, Hattori A. The oxytocinase subfamily of M1 aminopeptidases. *Biochim Biophys Acta* (2005) 1751(1):9–18. doi:10.1016/j.bbapap.2004.09.011
4. Saveanu L, Carroll O, Weimershaus M, Guermonprez P, Firat E, Lindo V, et al. IRAP identifies an endosomal compartment required for MHC class I cross-presentation. *Science* (2009) 325(5937):213–7. doi:10.1126/science.1172845
5. Serwold T, Gonzalez F, Kim J, Jacob R, Shastri N. ERAAP customizes peptides for MHC class I molecules in the endoplasmic reticulum. *Nature* (2002) 419(6906):480–3. doi:10.1038/nature01074
6. York IA, Chang SC, Saric T, Keys JA, Favreau JM, Goldberg AL, et al. The ER aminopeptidase ERAP1 enhances or limits antigen presentation by trimming epitopes to 8-9 residues. *Nat Immunol* (2002) 3(12):1177–84. doi:10.1038/ni860
7. Hammer GE, Gonzalez F, Champsaur M, Cado D, Shastri N. The aminopeptidase ERAAP shapes the peptide repertoire displayed by major histocompatibility complex class I molecules. *Nat Immunol* (2006) 7(1):103–12. doi:10.1038/ni1286
8. Yan J, Parekh VV, Mendez-Fernandez Y, Olivares-Villagomez D, Dragovic S, Hill T, et al. In vivo role of ER-associated peptidase activity in tailoring peptides for presentation by MHC class Ia and class Ib molecules. *J Exp Med* (2006) 203(3):647–59. doi:10.1084/jem.20052271
9. York IA, Brehm MA, Zendzian S, Towne CF, Rock KL. Endoplasmic reticulum aminopeptidase 1 (ERAP1) trims MHC class I-presented peptides in vivo and plays an important role in immunodominance. *Proc Natl Acad Sci U S A* (2006) 103(24):9202–7. doi:10.1073/pnas.0603095103
10. Blanchard N, Kanaseki T, Escobar H, Delebecque F, Nagarajan NA, Reyes-Vargas E, et al. Endoplasmic reticulum aminopeptidase associated with antigen processing defines the composition and structure of MHC class I peptide repertoire in normal and virus-infected cells. *J Immunol* (2010) 184(6):3033–42. doi:10.4049/jimmunol.0903712
11. Falk K, Rotzschke O, Rammensee HG. Cellular peptide composition governed by major histocompatibility complex class I molecules. *Nature* (1990) 348(6298):248–51. doi:10.1038/348248a0
12. Rotzschke O, Falk K, Deres K, Schild H, Norda M, Metzger J, et al. Isolation and analysis of naturally processed viral peptides as recognized by cytotoxic T cells. *Nature* (1990) 348(6298):252–4. doi:10.1038/348252a0

13. Elliott T, Townsend A, Cerundolo V. Antigen presentation. Naturally processed peptides. *Nature* (1990) 348(6298):195–7. doi:10.1038/348195a0
14. Rawlings ND, Barrett AJ, Bateman A. MEROPS: the database of proteolytic enzymes, their substrates and inhibitors. *Nucleic Acids Res* (2012) 40(Database issue):D343–50. doi:10.1093/nar/gkr987
15. Chang SC, Momburg F, Bhutani N, Goldberg AL. The ER aminopeptidase, ERAP1, trims precursors to lengths of MHC class I peptides by a "molecular ruler" mechanism. *Proc Natl Acad Sci U S A* (2005) 102(47):17107–12. doi:10.1073/pnas.0500721102
16. Evnouchidou I, Momburg F, Papakyriakou A, Chroni A, Leondiadis L, Chang SC, et al. The internal sequence of the peptide-substrate determines its N-terminus trimming by ERAP1. *PLoS One* (2008) 3(11):e3658. doi:10.1371/journal.pone.0003658
17. Nguyen TT, Chang SC, Evnouchidou I, York IA, Zikos C, Rock KL, et al. Structural basis for antigenic peptide precursor processing by the endoplasmic reticulum aminopeptidase ERAP1. *Nat Struct Mol Biol* (2011) 18(5):604–13. doi:10.1038/nsmb.2021
18. Kanaseki T, Blanchard N, Hammer GE, Gonzalez F, Shastri N. ERAAP synergizes with MHC class I molecules to make the final cut in the antigenic peptide precursors in the endoplasmic reticulum. *Immunity* (2006) 25(5):795–806. doi:10.1016/j.immuni.2006.09.012
19. Reeves E, Edwards CJ, Elliott T, James E. Naturally occurring ERAP1 haplotypes encode functionally distinct alleles with fine substrate specificity. *J Immunol* (2013) 191(1):35–43. doi:10.4049/jimmunol.1300598
20. Chen H, Li L, Weimershaus M, Evnouchidou I, van Endert P, Bouvier M. ERAP1-ERAP2 dimers trim MHC I-bound precursor peptides; implications for understanding peptide editing. *Sci Rep* (2016) 6:28902. doi:10.1038/srep28902
21. Infantes S, Samino Y, Lorente E, Jimenez M, Garcia R, Del Val M, et al. Cutting edge: H-2L(d) class I molecule protects an HIV N-extended epitope from in vitro trimming by endoplasmic reticulum aminopeptidase associated with antigen processing. *J Immunol* (2010) 184(7):3351–5. doi:10.4049/jimmunol.0901560
22. Stratikos E, Stern LJ. Antigenic peptide trimming by ER aminopeptidases – insights from structural studies. *Mol Immunol* (2013) 55(3–4):212–9. doi:10.1016/j.molimm.2013.03.002
23. Kochan G, Krojer T, Harvey D, Fischer R, Chen L, Vollmar M, et al. Crystal structures of the endoplasmic reticulum aminopeptidase-1 (ERAP1) reveal the molecular basis for N-terminal peptide trimming. *Proc Natl Acad Sci U S A* (2011) 108(19):7745–50. doi:10.1073/pnas.1101262108
24. Birtley JR, Saridakis E, Stratikos E, Mavridis IM. The crystal structure of human endoplasmic reticulum aminopeptidase 2 reveals the atomic basis for distinct roles in antigen processing. *Biochemistry* (2012) 51(1):286–95. doi:10.1021/bi201230p

25. Zervoudi E, Saridakis E, Birtley JR, Seregin SS, Reeves E, Kokkala P, et al. Rationally designed inhibitor targeting antigen-trimming aminopeptidases enhances antigen presentation and cytotoxic T-cell responses. *Proc Natl Acad Sci U S A* (2013) 110(49):19890–5. doi:10.1073/pnas.1309781110

26. Mpakali A, Giastas P, Mathioudakis N, Mavridis IM, Saridakis E, Stratikos E. Structural basis for antigenic peptide recognition and processing by endoplasmic reticulum (ER) aminopeptidase 2. *J Biol Chem* (2015) 290(43):26021–32. doi:10.1074/jbc.M115.685909

27. Hermans SJ, Ascher DB, Hancock NC, Holien JK, Michell BJ, Chai SY, et al. Crystal structure of human insulin-regulated aminopeptidase with specificity for cyclic peptides. *Protein Sci* (2015) 24(2):190–9. doi:10.1002/pro.2604

28. Mpakali A, Saridakis E, Harlos K, Zhao Y, Papakyriakou A, Kokkala P, et al. Crystal structure of insulin-regulated aminopeptidase with bound substrate analogue provides insight on antigenic epitope precursor recognition and processing. *J Immunol* (2015) 195(6):2842–51. doi:10.4049/jimmunol.1501103

29. Mpakali A, Saridakis E, Harlos K, Zhao Y, Kokkala P, Georgiadis D, et al. Ligand-induced conformational change of insulin-regulated aminopeptidase: insights on catalytic mechanism and active site plasticity. *J Med Chem* (2017) 60(7):2963–72. doi:10.1021/acs.jmedchem.6b01890

30. Kyrieleis OJ, Goettig P, Kiefersauer R, Huber R, Brandstetter H. Crystal structures of the tricorn interacting factor F3 from thermoplasma acidophilum, a zinc aminopeptidase in three different conformations. *J Mol Biol* (2005) 349(4):787–800. doi:10.1016/j.jmb.2005.03.070

31. Santiago C, Mudgal G, Reguera J, Recacha R, Albrecht S, Enjuanes L, et al. Allosteric inhibition of aminopeptidase N functions related to tumor growth and virus infection. *Sci Rep* (2017) 7:46045. doi:10.1038/srep46045

32. Stamogiannos A, Maben Z, Papakyriakou A, Mpakali A, Kokkala P, Georgiadis D, et al. Critical role of interdomain interactions in the conformational change and catalytic mechanism of endoplasmic reticulum aminopeptidase 1. *Biochemistry* (2017) 56(10):1546–58. doi:10.1021/acs.biochem.6b01170

33. Pierce LC, Salomon-Ferrer R, Augusto FdOC, McCammon JA, Walker RC. Routine access to millisecond time scale events with accelerated molecular dynamics. *J Chem Theory Comput* (2012) 8(9):2997–3002. doi:10.1021/ct300284c

34. Stamogiannos A, Koumantou D, Papakyriakou A, Stratikos E. Effects of polymorphic variation on the mechanism of endoplasmic reticulum aminopeptidase 1. *Mol Immunol* (2015) 67(2 Pt B):426–35. doi:10.1016/j.molimm.2015.07.010

35. Lopez de Castro JA, Alvarez-Navarro C, Brito A, Guasp P, Martin-Esteban A, Sanz-Bravo A. Molecular and pathogenic effects of endoplasmic reticulum aminopeptidases ERAP1 and ERAP2 in MHC-I-associated inflammatory disorders: towards a unifying view. *Mol Immunol* (2016) 77:193–204. doi:10.1016/j.molimm.2016.08.005

36. Brown MA, Kenna T, Wordsworth BP. Genetics of ankylosing spondylitis – insights into pathogenesis. *Nat Rev Rheumatol* (2016) 12(2):81–91. doi:10.1038/nrrheum.2015.133

37. Cortes A, Pulit SL, Leo PJ, Pointon JJ, Robinson PC, Weisman MH, et al. Major histocompatibility complex associations of ankylosing spondylitis are complex and involve further epistasis with ERAP1. *Nat Commun* (2015) 6:7146. doi:10.1038/ncomms8146

38. Hinks A, Martin P, Flynn E, Eyre S, Packham J; Childhood Arthritis Prospective Study-CAPS, et al. Subtype specific genetic associations for juvenile idiopathic arthritis: ERAP1 with the enthesitis related arthritis subtype and IL23R with juvenile psoriatic arthritis. *Arthritis Res Ther* (2011) 13(1):R12. doi:10.1186/ar3235

39. Kirino Y, Bertsias G, Ishigatsubo Y, Mizuki N, Tugal-Tutkun I, Seyahi E, et al. Genome-wide association analysis identifies new susceptibility loci for Behcet's disease and epistasis between HLA-B*51 and ERAP1. *Nat Genet* (2013) 45(2):202–7. doi:10.1038/ng.2520

40. Franke A, McGovern DP, Barrett JC, Wang K, Radford-Smith GL, Ahmad T, et al. Genome-wide meta-analysis increases to 71 the number of confirmed Crohn's disease susceptibility loci. *Nat Genet* (2010) 42(12):1118–25. doi:10.1038/ng.717

41. Kuiper JJ, Van Setten J, Ripke S, Van 't Slot R, Mulder F, Missotten T, et al. A genome-wide association study identifies a functional ERAP2 haplotype associated with birdshot chorioretinopathy. *Hum Mol Genet* (2014) 23(22):6081–7. doi:10.1093/hmg/ddu307

42. Tsoi LC, Spain SL, Knight J, Ellinghaus E, Stuart PE, Capon F, et al. Identification of 15 new psoriasis susceptibility loci highlights the role of innate immunity. *Nat Genet* (2012) 44(12):1341–8. doi:10.1038/ng.2467

43. Strange A, Capon F, Spencer CC, Knight J, Weale ME, Allen MH, et al. A genome-wide association study identifies new psoriasis susceptibility loci and an interaction between HLA-C and ERAP1. *Nat Genet* (2010) 42(11):985–90. doi:10.1038/ng.694

44. Cheng H, Li Y, Zuo XB, Tang HY, Tang XF, Gao JP, et al. Identification of a missense variant in LNPEP that confers psoriasis risk. *J Invest Dermatol* (2014) 134(2):359–65. doi:10.1038/jid.2013.317

45. Stratikos E, Stamogiannos A, Zervoudi E, Fruci D. A role for naturally occurring alleles of endoplasmic reticulum aminopeptidases in tumor immunity and cancer pre-disposition. *Front Oncol* (2014) 4:363. doi:10.3389/fonc.2014.00363

46. Mehta AM, Jordanova ES, Corver WE, van Wezel T, Uh HW, Kenter GG, et al. Single nucleotide polymorphisms in antigen processing machinery component ERAP1 significantly associate with clinical outcome in cervical carcinoma. *Genes Chromosomes Cancer* (2009) 48(5):410–8. doi:10.1002/gcc.20648

47. Evnouchidou I, Kamal RP, Seregin SS, Goto Y, Tsujimoto M, Hattori A, et al. Coding single nucleotide polymorphisms of endoplasmic reticulum aminopeptidase 1 can affect antigenic peptide generation in vitro by influencing basic enzymatic properties of the enzyme. *J Immunol* (2011) 186(4):1909–13. doi:10.4049/jimmunol.1003337

48. Reeves E, Colebatch-Bourn A, Elliott T, Edwards CJ, James E. Functionally distinct ERAP1 allotype combinations distinguish individuals with ankylosing spondylitis. *Proc Natl Acad Sci U S A* (2014) 111(49):17594–9. doi:10.1073/pnas.1408882111

49. Evnouchidou I, Birtley J, Seregin S, Papakyriakou A, Zervoudi E, Samiotaki M, et al. A common single nucleotide polymorphism in endoplasmic reticulum aminopeptidase 2 induces a specificity switch that leads to altered antigen processing. *J Immunol* (2012) 189(5):2383–92. doi:10.4049/jimmunol.1200918

50. Goto Y, Hattori A, Ishii Y, Tsujimoto M. Reduced activity of the hypertension-associated Lys528Arg mutant of human adipocyte-derived leucine aminopeptidase (A-LAP)/ER-aminopeptidase-1. *FEBS Lett* (2006) 580(7):1833–8. doi:10.1016/j.febslet.2006.02.041

51. Martin-Esteban A, Gomez-Molina P, Sanz-Bravo A, Lopez de Castro JA. Combined effects of ankylosing spondylitis-associated ERAP1 polymorphisms outside the catalytic and peptide-binding sites on the processing of natural HLA-B27 ligands. *J Biol Chem* (2014) 289(7):3978–90. doi:10.1074/jbc.M113.529610

52. Sui L, Gandhi A, Guo HC. Crystal structure of a polypeptide's C-terminus in complex with the regulatory domain of ER aminopeptidase 1. *Mol Immunol* (2016) 80:41–9. doi:10.1016/j.molimm.2016.10.012

53. Gandhi A, Lakshminarasimhan D, Sun Y, Guo HC. Structural insights into the molecular ruler mechanism of the endoplasmic reticulum aminopeptidase ERAP1. *Sci Rep* (2011) 1:186. doi:10.1038/srep00186